INVESTIGATION AND ANALYSIS OF BIFACIAL PHOTOVOLTAICS MODULES WITH REFLECTIVE LAYER

Ernest SNG[1,2], Chong Xian ANG[1], Idris Li Hong LIM[1]
[1] University of Glasgow, University Avenue, Glasgow G12 8QQ, UK
[2] REC Solar Pte Ltd, 20 Tuas South Ave 14, Singapore 637312, Singapore
Contact: ernest.sng@recgroup.com

ABSTRACT: While the analysis of optical gains and power transfer of monofacial photovoltaics module are relatively well established, there are many nuanced effects that contribute to bifacial cell to module power transfer. To improve the bifacial module power during indoor flash test, reflective layers had been included in the inter-cell spacing. This reflective layer improves bifacial module STC maximum power point (Pmpp) and current. This paper presents the investigation and analysis of bifacial PV modules with reflective layer at the inter-cell spacing. Three main bifacial module configurations with reflective layer are studied where the reflective surface was inserted at different positions, (1) behind the rear glass or transparent back sheet, (2) in between the glass and encapsulant, and (3) in between the encapsulant. A numerical model is created to simulate the current gain from each configuration with varying inter-cell spacing with varying illumination positions.
Keywords: Bifacial, PV Module, Ray Tracing

1 INTRODUCTION

Photovoltaic (PV) energy sources could achieve grid parity with traditional energy sources by either cost reduction or increase in efficiency with new technology. Currently the cost of PV modules had exponentially reduced due to improvement in manufacturability, economic of scale, and improved technology. Traditionally, the implementation of new technology had always been associated with an increase in cost. For PV manufacturers to achieve the grid parity goal, new technology implemented had to be cost effective and reliable. One such potential technology enabler to lower the cost of PV is the bifacial PV cells.

In a typical solar cell, light is only collected from the front side of the cell. Bifacial PV cells enable the collection of light from the both side of the cell, thus generating additional power in the same photovoltaics module [1][2]. By generating more power at lower cost, bifacial design enables PV energy sources to be attractive to consumers. Through the changing of module materials in the construction of bifacial PV modules, an increase of energy yield is achieved without a large increase in cost [3].

Bifacial PV cells can be encapsulated into the typical monofacial solar module structure, which has cells sandwiched between the encapsulant with glass on the front side and white back sheet on the rear, as shown in Figure 1 Bifacial cells in monofacial moduleFigure 1. While bifacial modules come in a few different structures, the standard bifacial module in Figure 2 of glass/glass or glass/transparent back sheet could capture additional sunlight to the rear from ground reflectance [4][5][6]. However, without the white back sheet like of monofacial solar module that is contributing to module internal reflectance [7], the transmission of light during STC results in the power loss as compared to the monofacial modules with the white back sheet on the rear [8].

Recent developments of bifacial modules with a reflective layer inserted between the cell increase the module front side current without totally removing the bifacial capability of the module [8][9]. In this structure, various configurations of varying locations of the reflective surface were proposed. The three main configurations differs where the reflective surface was inserted: (1) behind the rear glass or transparent back sheet in Figure 3, (2) in between the glass and encapsulant in Figure 4, and (3) in between the encapsulant in Figure 5. In the monofacial module structure and bifacial module structure with reflective layer of configuration 1 and 2, the incoming light from the front of the module is reflected onto both the front and rear of the cell. The light ray traces are shown in Figure 1, Figure 3, and Figure 4 with arrows marked "A". The standard bifacial module structure and all three bifacial module structures with reflective layer allows the ground reflectance to be capture by the rear of the active cell, as shown in Figures 2 to 5. The location of the reflective layer determines the amount of ground reflectance reaching the cell.

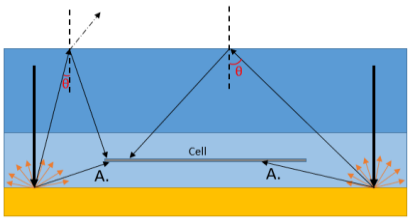

Figure 1 Bifacial cells in monofacial module

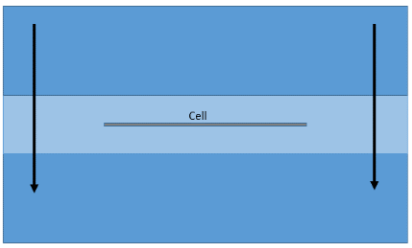

Figure 2 Standard bifacial module

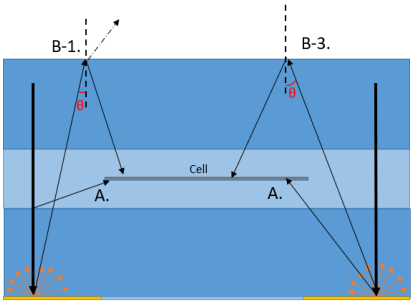

Figure 3 Bifacial module reflective layer configuration 1

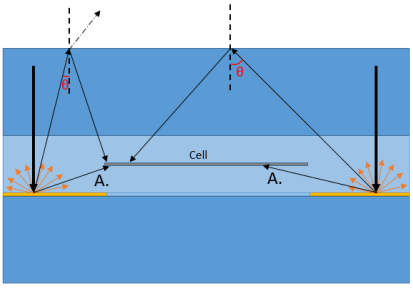

Figure 4 Bifacial module reflective layer configuration 2

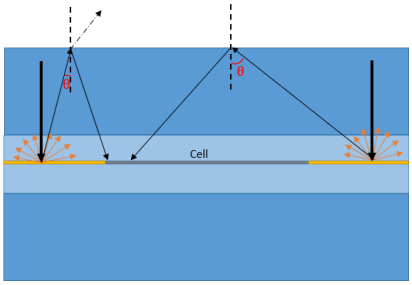

Figure 5 Bifacial module reflective layer configuration 3

The influence of the cell gap to monofacial cells in monofacial modules were widely reported. With wider cell gap, the reflectivity area increases and in turn the cell current [7][10][11]. For bifacial cell and module, strategic placement of the reflective surface affects the module performance during STC and outdoor monitoring.

In this paper, the front and rear current of the bifacial module structures highlighted above will first be analyzed. The equations on light scattering and probability of collection by the active cell area are first modelled with optical ray trace. Next, physical measurements performed on the materials are provided as inputs into the numerical model.

The rest of this paper is organized as follows: Section 2 provides the development of the numerical model with the optical ray trace. Simulation results of the different configurations will be discussed in Section 3. A parametric study on the varying inter-cell gap with reflective layer will be presented. This will be followed by the discussion and analysis of the performance of each configuration. Conclusions are presented in Section 5.

2 METHODOLOGY OF SIMULATION

2.1 Assumptions and experimental inputs

Firstly, some assumptions of the refractive index of the materials were made. The glass and encapsulant refractive index are assumed to be the same, as the optical loss through reflection at this particular junction is very small and can be negligible [12]. The refractive index of glass and encapsulant is set at 1.5 and the refractive index of air is set at 1 [7][12].

Secondly, it is considered that the reflective layer will scatter the light that falls on it into different directions. In order to cover all possible directions of the scattered light, the directions are divided into two segments which is the azimuth and polar directions. The assumption of the direction of light was made the same such that it is scattered uniformly at interval of 3 degrees in the polar coordinates and at intervals of 6 degrees in the azimuth coordinates, resulting in a total of 3600 rays. The reflected rays were also assumed to be unpolarized, thus consisting of parallel and perpendicular light.

Lastly, the white area is divided into unit areas of $1mm^2$ which reflects an individual ray into each unit area of the module. Two experiment inputs were essential for the numerical model were measured by spectrometer, the normalized reflected radiant intensity and the reflectance of the reflective layer. The wavelength of 632nm was chosen to represent the angular scattering of the spectrum AM1.5G on the reflective layer. Its weighted average reflectance is also calculated with respect the AM1.5G spectrum.

2.2 Equations

When light falls on the white area, it will be scatted into different directions. However, the intensity of the scattered light will vary according to the reflectivity of the white inter-cell gap. The calculation of the irradiance at certain direction can be calculated using Equation (1) [7][8]. where irradiance at a certain direction, S(θ) is reflected by the back-sheet where aue is the unit area of the back sheet, Φp is the Power of incident light per unit area, WARbs is the back sheet weighted Average Reflectance, Sn(θ) is the measured normalized reflected radiant intensity of the back sheet, θ is the polar angle, and φ is the azimuth angle.

$$S(\theta) = \text{aue}.\Phi\text{p}\,.(\text{WARbs})\frac{\text{Sn}(\theta)}{\iint \text{Sn}(\theta)\sin\theta d\varphi d\theta} \quad (1)$$

The white inter-cell gap will reflect off the ray that incident on it into different directions. Rays will either transmit out of the module or reflected internally inside. A matrix consisting of the coordinated of the module had been simulated to determine the possible locations of the reflected rays. Some assumptions made are the uniform separation of scatted rays across the polar and azimuth angle, and the non-contribution of cells irradiance after two bounces. The contribution of reflected light that hits the rear side of the cell the position vector of the ray are computed by the Equations (2) and (3) [7][8], where t_1 is the thickness of rear encapsulant .For those rays that were not scattered to the rear of the cell and which were reflected by front glass back to the cell, Equations (4) and (5) were applied, where t_2 and g are the thickness of front encapsulant and glass respectively. For incident angle more than critical angle of 41.8°, total internal reflection is considered. If the angle of incident is less than the critical angle of air/glass (41.8°) the reflectance and transmittance radiant intensity are calculated with Fresnel equation.

$$x2 = x1 + (t_1) * \tan(\theta)\cos(\varphi) \quad (2)$$

$$y2 = y2 + (t_1) * \tan(\theta)\sin(\varphi) \quad (3)$$

$$x3 = x1 + (2g + t_1 + 2t_2) * \tan(\theta)\cos(\varphi) \quad (4)$$

$$y3 = y1 + (2g + t_1 + 2t_2) * \tan(\theta)\sin(\varphi) \quad (5)$$

As discussed earlier, the irradiance reflected by the back sheet and incident on the rear of the cell could be calculated if x2 and y2 is situated on the cell with Equations (6) and (7) for the ray reflected to the rear and front of the cell respectively [7, 8, 13].

$$P_r = \int_{q1}^{q2}\int_{p1}^{p2}\int_{0}^{\pi}\int_{\alpha}^{\frac{\pi}{2}} S(\theta).T1(x2,y2).R_g.d\theta\, d\varphi\, dx\, dy \quad (6)$$

$$P_f = \int_{q1}^{q2}\int_{p1}^{p2}\int_{0}^{\pi}\int_{0}^{\alpha} S(\theta).T1(x3,y3).R_g\, d\theta d\phi dx dy \quad (7)$$

The current gain calculated by the numerical model includes the reflectance of the back sheet and the internal scattering. However, only two bounces were considered for the calculation as it was assumed that radiant intensity would be negligible after two bounces. This assumption could be further investigated by calculating the absorption in glass and EVA. The EVA encapsulant are typically of the same refractive index as glass, in order to reduce losses. Hence, the absorption losses of light, $\alpha_{medium}(\lambda)$, traversing in the glass and EVA could be calculated using Equation (8), where the power of the incident light is Φp (λ). The absorption coefficient of the medium is described in Equation (9), where t is the layer thickness, and θ is the angle of propagation. This equation could be applied to both glass and encapsulant collectively.

$$\alpha_{medium}(\lambda) = \frac{reflected\ (\lambda) + transmitted\ (\lambda)}{incident\ light\ (\lambda)} \quad (8)$$

$$Absorption_{medium}(\lambda) = \Phi p\ (\lambda)[1 - e^{-\alpha_{medium}(\lambda)t}] \quad (9)$$

Equation (10) calculates the current gain from the reflective area to the rear of the bifacial cell for the monofacial module structure and bifacial module structure with reflective layer of Configurations 1 and 2. Equation (11) calculates the current gain from the reflective area to the front of the cell and Equation (12) calculates the total current gain to the cell from the reflective area.

$$Current_{\text{gain rear}} = \frac{\left(\frac{I_{sc.r}}{I_{sc.f}}\right) * P_r}{\Phi p\ .\text{cell area}} \quad (10)$$

$$Current_{\text{gain front}} = \frac{P_f}{\Phi p\ .\text{cell area}} \quad (11)$$

$$Current_{\text{gain}} = \frac{P_{f+\left(\frac{I_{sc.r}}{I_{sc.f}}\right)*P_{rear}}}{\Phi p\ .\text{cell area}} \quad (12)$$

3 RESULT AND DISCUSSIONS

3.1 Front illumination current gain comparison

The simulated current gains with and without consideration of absorption with varying inter-cell gap of the three different bifacial module structure with reflective layer configuration as illustrated in Figure 3, Figure 4, and Figure 5 where discussed in this section. From Figure 6 the current gain reduces from Configuration 1 to Configuration 3. Difference between the three configurations is the distance between the reflective layer to the cell.

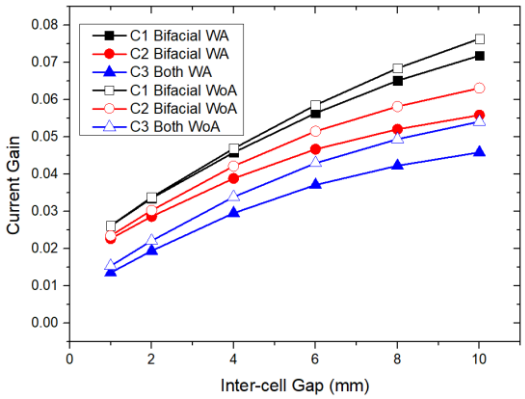

Figure 6 Current gain of bifacial modules for three configurations (C1, C2, C3) with (WA) & without (WoA) absorption

The additional distance between the reflective layer and the cell increases the number of rays being reflected onto the cell. In the illustration of all the bifacial modules configuration cross section, the distance travelled by the rays absorbed on the front side is twice as compared to those absorbed by the rear. In Figure 6 the difference between the current gain with and without consideration of absorption loss could be used to explain the contributions of front and rear to the current gain. Similarly, this is seen in Figure 7 where the current gain is breakdown into front and rear. Configuration 3 has no contributions from the rear as the reflective layer is on the same plane as the cell. Whereas Configuration 2 has minimum rear contribution with increasing cell gap as most light rays are reflected towards the front glass as compared to Configuration 1. At inter-cell gap of 1mm to 10mm, Configuration 1 has the highest current gain of the three. Configuration 1 has the highest rear current gain from the rear surpassing Configuration 2 rear current across 1mm to 10mm. With front illumination, Configuration 1 rear current gain exceeds configuration 2 and 3 front current gain. A higher current gain could be achieved for Configuration 1 if the bifaciality factor of the cell improves. Currently, bifaciality factor of 0.8 was used for Equation (10) for this model.

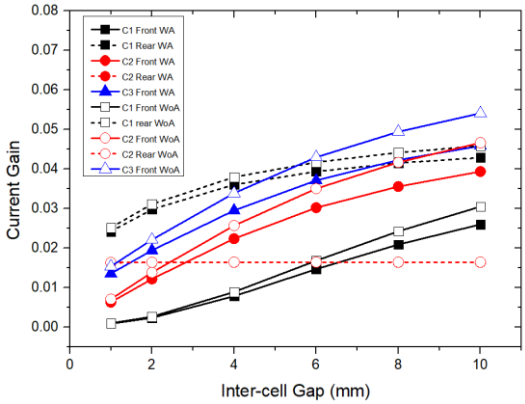

Figure 7 Rear and front current gain of bifacial modules for three configurations

3.2 Rear illumination current gain comparison

While Configuration 1 has highest current gain for front side illumination, there would be little current gain from rear illumination as all the light rays that are incident on the inter-cell gap are reflected out of the module. Configuration 2 and 3, light rays would reflected to the rear of the cell as illustrated in Figure 8 and Figure 9.

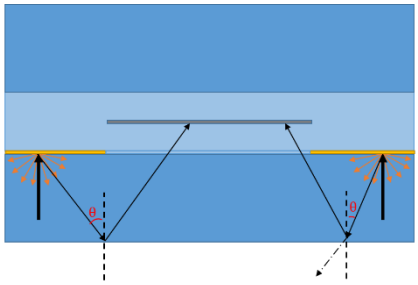

Figure 8 Configuration 2 rear illumination

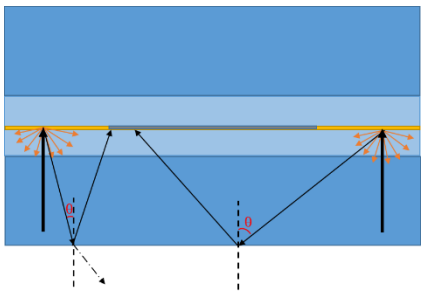

Figure 9 Configuration 3 rear illumination

Figure 10 plots the simulated current gain with rear illumination with Configuration 2 and 3. As the reflective layer distance from the cell between the two configurations are not significant, the resulted current gain is comparative close.

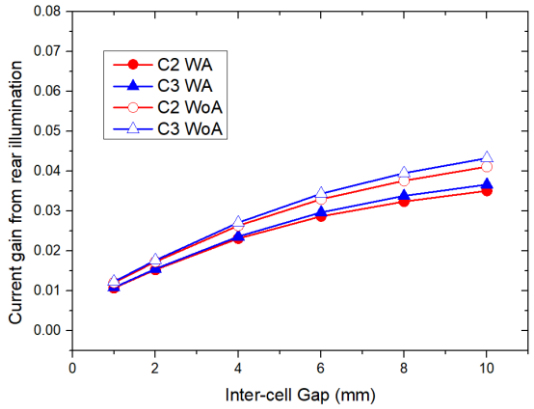

Figure 10 Current gain front rear illumination

3.3 Double sided illumination comparison on bifacial and monofacial cell

While the results discussed previously, Configuration 1 to have the highest current gain during standard testing condition indoor flash test with front side illumination. However, bifacial modules are illuminated on both sides during outdoor energy yield. Therefore, the three bifacial module configurations are simulated for both sided illumination. Adding on the results of front side and rear side illumination current gain, Configuration 2 and 3 surpass Configuration 1 current gain. The front and rear current gain for Configuration 2 results in the highest current gain across 1mm to 10mm inter-cell gap distance. This leads to the disparity between indoor and outdoor performance for the different module configurations

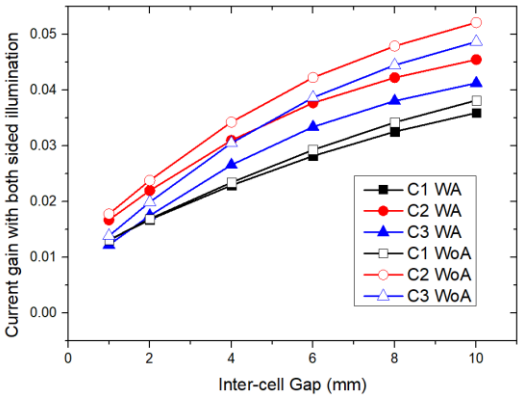

Figure 11 Current gain with both sided illumination

In monofacial modules, reflective rear encapsulants that are on the same plane as the cells are used to reduced absorption losses as the light rays are reflected on the same plane as the cell. Additionally, this remove the possibility of rays being reflected onto the inactive rear of a monofacial cell. In Figure 12, the three configurations were compared

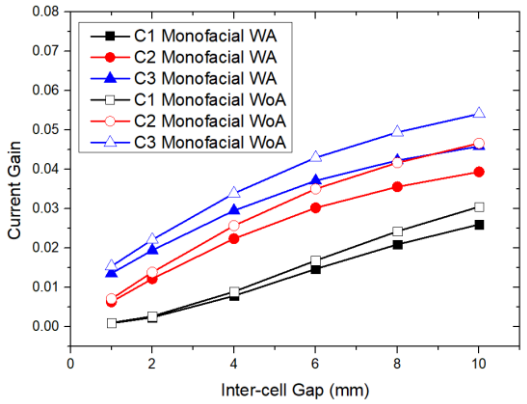

Figure 12 Current gain of monofacial modules for three configurations from front illumination

To compare the reflective layers effect on both monofacial and bifacial modules during pseudo outdoor conditions, a both sided illumination was used to simulate the current gain for monofacial modules shown in Figure 13. While Configuration 2 has the highest current gain across 1mm to 10mm inter-cell gap, Configuration 1 and 3 has little different at a typical 2mm inter-cell gap. The outdoor energy yield of bifacial module would exceed monofacial modules, however the outdoor performance is still not as distant between the bifacial modules.

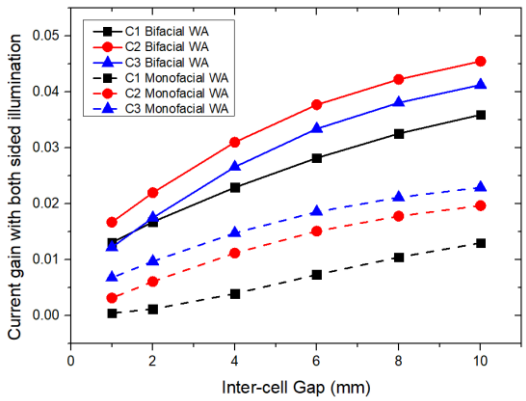

Figure 13 Current gain for monofacial and bifacial modules with both sided illumination

For front side illumination shown in Figure 6, at 2mm inter-cell gap it has been shown that Configuration 1 has the highest current gain of 3.4%. In comparison, for the monofacial module group Configuration 3 has the highest the current gain at 1.9% with front side illumination which is half of the bifacial modules. For the rear illumination, Configuration 2 and 3 has comparable gain while Configuration 1 has no additional gain as the reflective layer reflects the rays out of the module. In outdoor energy yield setting the modules are illuminated on both sides, this results the change in current gain for bifacial modules Configuration 1 to 1.7%, Configuration 2 to have 2.2%, and Configuration 3 to 1.8%. In addition, the simulation results show most of the current gain for bifacial modules with 2mm inter-cell gap comes from the rear of the cell from front side illumination.

4 CONCLUSION

This paper discussed three main bifacial module configurations with reflective layer at different positions are studied in detail; namely Configuration 1: Glass/EVA/ Bifacial Solar Cell/EVA/Glass/Reflective Layer, Configuration 2: Glass/EVA/ Bifacial Solar Cell/EVA/Reflective Layer /Glass, and Configuration 3: Glass/EVA/ Reflective Layer/ Bifacial Solar Cell/EVA /Glass. Optical ray trace model for the three configurations was created with inputs from test measurements. The simulation on the three numerical models created takes into consideration of absorption loss to simulate the current gain from each configuration with varying inter-cell spacing. The corresponding performance gain was evaluated for models with and without absorption loss From the simulated results, the optimal configuration for bifacial cell considering absorption losses in the module materials is proposed.

7 REFERENCES

[1] A. Cuevas, A. Luque, J. Eguren, and J. del Alamo, “50 Per cent more output power from an albedo-collecting flat panel using bifacial solar cells,” *Sol. Energy*, vol. 29, no. 5, pp. 419–420, Jan. 1982.

[2] G. J. M. Janssen, B. B. Van Aken, A. J. Carr, and A. A. Mewe, “Outdoor Performance of Bifacial Modules by Measurements and Modelling,” *Energy Procedia*, vol. 77, pp. 364–373, Aug. 2015.

[3] R. Guerrero-Lemus, R. Vega, T. Kim, A. Kimm, and L. E. Shephard, “Bifacial solar photovoltaics – A technology review,” *Renew. Sustain. Energy Rev.*, vol. 60, pp. 1533–1549, Jul. 2016.

[4] S. Guo, T. M. Walsh, and M. Peters, “Vertically mounted bifacial photovoltaic modules: A global analysis,” *Energy*, vol. 61, pp. 447–454, Nov. 2013.

[5] U. A. Yusufoglu *et al.*, “Simulation of Energy Production by Bifacial Modules with Revision of Ground Reflection,” *Energy Procedia*, vol. 55, pp. 389–395, 2014.

[6] S. Wang *et al.*, “Bifacial Photovoltaic Systems Energy Yield Modelling,” *Energy Procedia*, vol. 77, pp. 428–433, 2015.

[7] S. Guo *et al.*, “Investigation of the short-circuit current increase for PV modules using halved silicon wafer solar cells,” *Sol. Energy Mater. Sol. Cells*, vol. 133, pp. 240–247, 2015.

[8] J. P. Singh, S. Guo, I. M. Peters, A. G. Aberle, and T. M. Walsh, “Comparison of Glass/Glass and Glass/ Backsheet PV Modules Using Bifacial Silicon Solar Cells,” *IEEE J. Photovoltaics*, vol. 5, no. 3, pp. 783–791, May 2015.

[9] J. A. M. van Roosmalen, S. L. Luxembourg, J. Liu, L. A. G. Okel, and B. B. Van Aken, “White Bifacial Modules – Improved STC Performance Combined with Bifacial Energy Yield,” *32nd Eur. Photovolt. Sol. Energy Conf. Exhib.*, pp. 42–47, Jul. 2016.

[10] W.-S. Su *et al.*, “Optimization of the output power by effect of backsheet reflectance and spacing between cell strings,” in *2011 37th IEEE Photovoltaic Specialists Conference*, 2011, pp. 003218–003220.

[11] M. B. Koentopp, M. Schu?tze, D. Buss, and R. Seguin, “Optimized Module Design: A Study of Encapsulation Losses and the Influence of Design Parameters on Module Performance,” *IEEE J. Photovoltaics*, vol. 3, no. 1, pp. 138–142, Jan. 2013.

[12] I. M. Peters, Y. S. Khoo, and T. M. Walsh, “Detailed Current Loss Analysis for a PV Module Made With Textured Multicrystalline Silicon Wafer Solar Cells,” *IEEE J. Photovoltaics*, vol. 4, no. 2, pp. 585–593, Mar. 2014.

[13] K. R. McIntosh, R. M. Swanson, and J. E. Cotter, “A simple ray tracer to compute the optical concentration of photovoltaic modules,” *Prog. Photovoltaics Res. Appl.*, vol. 14, no. 2, pp. 167–177, Mar. 2006.